K-shell ionization cross section of Ti and Cu atoms by 1 and 2 GeV electrons

IOP Publishing Journal of Physics B: Atomic, Molecular and Optical Physics
J. Phys. B: At. Mol. Opt. Phys. **XX** (XXXX) XXXXXX https://doi.org/XXXX/XXXX

K-shell ionization cross section of Ti and Cu atoms by 1 and 2 GeV electrons

R.M. Nazhmudinov[1,2], A.V. Shchagin[1,3], S.V. Trofymenko[3,4], I.A. Kishin[1,2], A.S. Kubankin[1,2], A.P. Potylitsyn[5], A.S. Gogolev[5], N.A. Filatov[5], G. Kube[6], N.A. Potylitsina-Kube[6], M. Stanitzki[6] and A. Novokshonov[6]

[1] Belgorod National Research University, Pobedy St. 85, 308015 Belgorod, Russia
[2] P.N. Lebedev Physical Institute of the Russian Academy of Sciences, Leninskiy Ave. 53, 119991 Moscow, Russia
[3] Kharkiv Institute of Physics and Technology, Akademichna St. 1, 61108 Kharkiv, Ukraine
[4] V.N. Karazin Kharkiv National University, Svobody Sq. 4, 61022 Kharkiv, Ukraine
[5] Tomsk Polytechnic University, Lenin Ave. 30, 634050, Tomsk, Russia
[6] Deutsches Elektronen-Synchrotron DESY, Notkestr. 85, 22607 Hamburg, Germany

E-mail: Ramazan.M.Nazhmudinov@gmail.com

Received xxxxxx
Accepted for publication xxxxxx
Published xxxxxx

Abstract

The *K*-shell ionization cross sections of titanium and copper atoms were determined by analysing the spectra of characteristic x-ray radiation generated by an electron beam with energies of 1 and 2 GeV in metal foils. New data obtained for these energies demonstrate the influence of the density effect on the ionization cross sections values. The results were compared with the previous experimental data and calculations based on pure theoretical and semi-empirical models.

Keywords: ionization cross section, relativistic electrons, density effect, electron-atomic collision, electron impact

1. Introduction

Information on inner shells ionization cross sections of atoms is necessary for fundamental research of electron-atomic collisions from low [1,2] to ultrahigh [3,4] energies, astrophysical phenomena [1,5], laser-solid interactions [6,7] and processes in plasma [2,5]. Data on the ionization cross sections are widely used in elemental and structural analysis (for example, in x-ray fluorescence and electron microprobe analyses or electron energy loss and Auger electron spectroscopies), calculation of radiation damage [8], and can also find application in the development of beam diagnostics systems (such as beam profile monitors of different types [9,10]) or laser-plasma sources of fast electrons. The values of ionization cross sections obtained by various authors may differ significantly despite the large number of measurements and calculations performed to date. Also the experimental data do not cover all the energies of incident particles required for solving fundamental and applied problems.

In addition, it is of interest to study the phenomenon of ionization cross section saturation. This saturation is due to the screening of the incident charged particles' electric field by polarized atoms of the medium (the so-called density effect). A theoretical model that takes into account the influence of the density effect on the *K*-shell ionization cross section was proposed by Dangerfield [11]. However, in subsequent experiments such saturation was not observed [12,13]. This "lack of the density effect" was experimentally and theoretically investigated in detail by Bak et al. [14,15], Sørensen [16], Chechin et al. [17], Meyerhof et al. [18], and Spooner et al. [19]. It was found that the reason why the

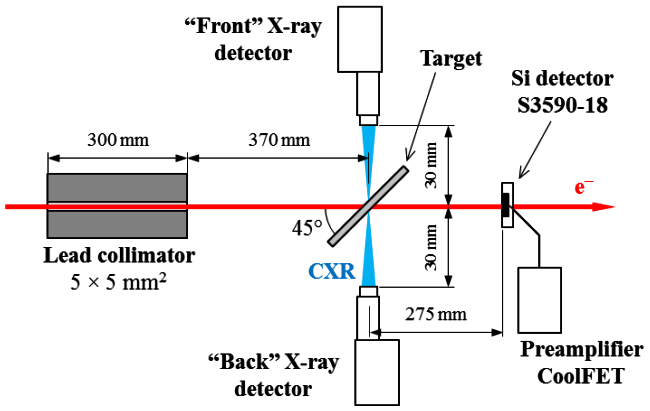

Figure 1. Experimental layout.

density effect had not been detected was related to the features of the measurements.

The yield of characteristic x-ray radiation (CXR) or Auger electrons generated by charged particle beams in a target (which is generally a thin film) is usually measured to determine the cross sections. When a charged particle crosses the entrance (front) surface of the target, transition radiation (TR) is generated and propagates along the beam axis additionally ionizing the target atoms. It increases the yield of CXR and Auger electrons (especially for the front side) and consequently leads to an overestimation of the measured cross section [15–19]. To minimize the effect of TR, Bak et al. [15] proposed measuring the radiation yield from the exit (back) surface of the target. In this case, the target volume acts as a filter that absorbs TR.

In this work, our preliminary experimental data concerned to titanium and copper atoms excited by 1 and 2 GeV electrons are described. The electron impact K-shell ionization cross sections were determined from the intensity of CXR. The spectra of CXR emitted from the front and back surfaces of the self-supporting foils were registered during the measurements.

2. Experiment

The experiment was performed at the Test Beam Facility TB21 of DESY [20]. The measurement scheme is shown in figure 1. The electron beam with energy E_0 of 1–2 GeV and intensity of 5.9×10^3 electrons per second passes in air through a 5×5 mm^2 square lead collimator and crosses the target, which is a metal foil located at an angle of 45° to the beam axis. Beam-induced spectra of CXR emitted from the front and back target surfaces are registered by two semiconductor x-ray detectors mounted perpendicular to the beam axis. The semiconductor silicon detector was installed behind the target, designed to measure the number of particles which passed through the target.

Titanium and copper foils of 51.3 ± 0.2 μm and 32.2 ± 0.1 μm thickness, respectively, were used as targets. The thickness of the foils was determined from attenuation of

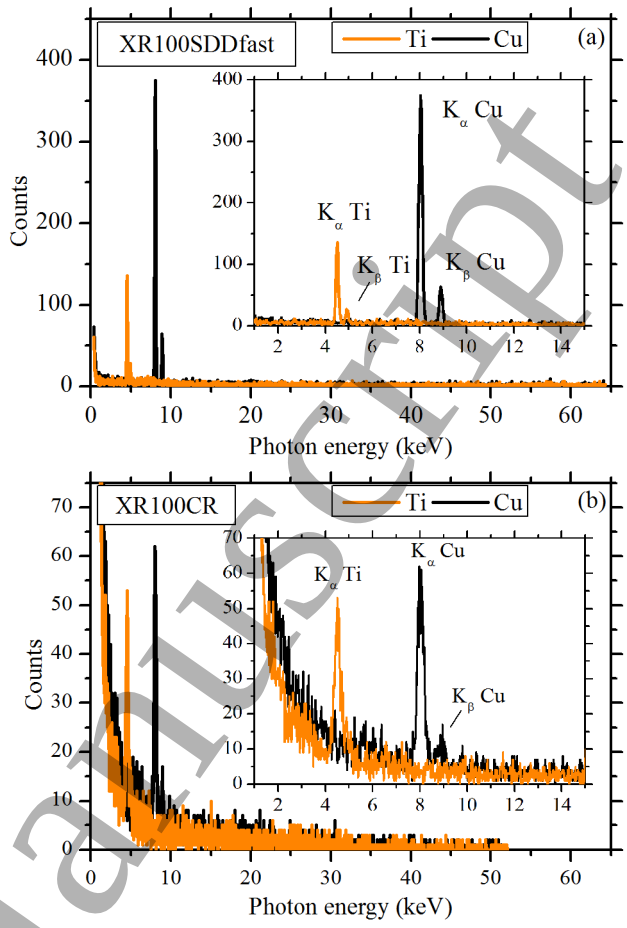

Figure 2. Typical x-ray spectra of titanium and copper targets, measured by (a) XR100SDDfast and (b) XR100CR semiconductor detectors at the beam energy of 2 GeV (the insets show the same spectra in the energy range 1–15 keV).

the characteristic x-ray L_α line of tungsten (8.396 keV) using an x-ray tube Oxford Instruments Apogee 5000 with tungsten anode.

Table 1. Main characteristics of the used x-ray detectors.

Characteristic	XR100SDDfast	XR100CR
Measured resolution at		
4.51 keV (Ti K_α)	125 eV	< 320 eV
8.04 keV (Cu K_α)	157 eV	< 320 eV
Detection efficiency at		
4.51 keV (Ti K_α)	98.6%	97.3%
4.93 keV (Ti K_β)	99.0%	97.9%
8.04 keV (Cu K_α)	99.7%	99.4%
8.90 keV (Cu K_β)	99.3%	99.1%
Input Be window		
area	17.0 mm^2	11.1 mm^2
thickness	12.5 μm	25.4 μm
Si crystal thickness	500 μm	500 μm

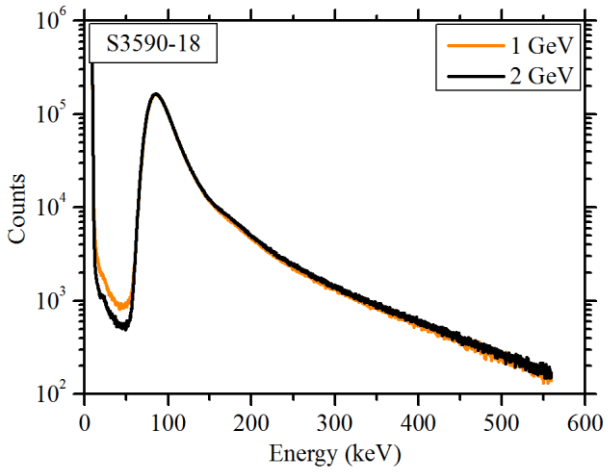

Figure 3. Ionization energy loss spectra of relativistic electrons measured by the silicon detector S3590-18.

The silicon drift detector XR100SDDfast and the silicon lithium detector XR100CR (both manufactured by Amptek) were used to measure the x-ray K_α and K_β lines intensity of titanium and copper. Detection efficiency at the corresponding photon energies for these detectors (their main characteristics are summarized in table 1) is close to 100% and is mainly determined by radiation absorption in the beryllium input windows. The x-ray detectors were installed on the distance of 30 mm from the target and made it possible to simultaneously register the spectra of radiation emitted from the front and back target surfaces (examples of the measured spectra are shown in figure 2).

The measured spectra contain sharp peaks of CXR corresponding to the K_α (4.51 keV) and K_β (4.93 keV) lines of titanium, as well as the K_α (8.04 keV) and K_β (8.90 keV) lines of copper [21]. The use of two detectors, both of which were mounted to the same plate along with the target, made it possible to obtain data corresponding to both target surfaces in a single measurement run. The selection of the observed target surface for each detector was carried out by rotating the plate by 180°.

The semiconductor silicon detector Hamamatsu S3590-18 with the crystal size of 10×10×0.3 mm^3 and the preamplifier Amptek CoolFET A250CF was used as a beam current monitor. Spectra measured with this detector contain the broad asymmetric peak with a maximum at 85.5 keV. This so-called Landau peak corresponds to the distribution of ionization energy loss of relativistic electrons in a silicon layer 300 μm thick, as shown in figure 3. The number of events in this peak, obtained by integrating the spectrum in the range from 46 to 550 keV, corresponds to the number of electrons passed through the target and the detector. The low number of events in the energy range 14–46 keV (about 1% of the peak area) indicates the absence of edge effects, which is due to the small transverse size of the electron beam (5 mm) compared to the size of the detector (10 mm) and the correct positioning of the detector relative to the beam axis. The intense signal below 14 keV is due to the noise of the spectroscopic system.

Signals from all three semiconductor detectors were processed in the Amptek PX5 digital pulse processors. For energy calibration of the detectors, CXR of the targets, as well as x-ray and γ-lines of the radioactive source ^{241}Am, were used. The spectroscopic system performance significantly exceeded the actual counting rate (100 times for the detector S3590-18 and more than 1000 times for the detectors XR100SDDfast and XR100CR) during the measurements. Thus, possible overloading of the detectors was excluded, which is confirmed by the absence of pile-ups in the measured spectra.

3. Results of measurements

3.1 Determination of the cross section values

The number of registered photons of the CXR *K*-lines and the number of electrons passing through the target allow one to determine the *K*-shell ionization cross section σ_K of the target atoms according to

$$\sigma_K = \frac{4\pi}{\sqrt{2}d\,\Omega n\omega_K}\frac{N_\gamma}{N_e}, \qquad (1)$$

where

$$N_\gamma = \sum_{i=\alpha,\beta} N_\gamma^i = \sum_{i=\alpha,\beta} \frac{\sqrt{2}d\,N_{\gamma\mathrm{exp}}^i}{T_{\mathrm{air}}^i \varepsilon^i \lambda^i (1-\exp[-\sqrt{2}d/\lambda^i])}, \qquad (2)$$

d is the target thickness, Ω is the solid angle of the detector, n is the concentration of the target atoms, ω_K is the *K-shell* fluorescence yield (0.218 ± 0.008 for titanium and 0.438 ± 0.016 for copper according to Yashoda et al. [22]), N_γ is the total number of CXR photons produced in the target by the electron beam, N_γ^i is the number of emitted photons of the K_α or K_β line, N_e is the number of electrons passing through the target, $N_{\gamma\mathrm{exp}}^i$ is the measured number of events in the CXR spectral peaks, T_{air}^i is the CXR transmittance through 30 mm air layer (taken from the reference [23]), ε^i is the detection efficiency (table 1), λ^i is the attenuation length for CXR propagating in the target [23], and the superscript i corresponds to the K_α and K_β lines of CXR.

3.2 Influence of the accompanying radiation

Radiation accompanying the electron beam can provide photoionization of the target atoms and provide an additional yield of CXR from the target. The accompanying radiation includes bremsstrahlung and CXR from the beam line equipment, synchrotron radiation from the selecting magnet, TR from the Kapton foil at the exit of the electron beam from vacuum to air, installed upstream of the lead collimator (the selecting magnet and the Kapton foil are not shown in figure 1), radiation from the inner walls of the lead collimator, and also TR from the front surface of the target.

Table 2. Measured *K*-shell ionization cross sections for titanium atoms (in barns).

E_0 (GeV)	XR100SDDfast front	XR100CR front	XR100SDDfast back	XR100CR back
1	1069 ± 93	951 ± 85	809 ± 72	696 ± 66
2	1186 ± 102	1187 ± 103	844 ± 74	934 ± 84
2	*1153 ± 99*	*1254 ± 108*	*840 ± 74*	*963 ± 86*

Table 3. Measured *K*-shell ionization cross sections for copper atoms (in barns).

E_0 (GeV)	XR100SDDfast front	XR100CR front	XR100SDDfast back	XR100CR back
1	869 ± 70	825 ± 66	335 ± 28	352 ± 30
2	914 ± 74	935 ± 74	368 ± 31	405 ± 34
2	*841 ± 68*			*426 ± 36*

To check the possible influence of accompanying radiation, additional measurements of the x-ray spectra were performed using x-ray filters. The filters consisted of foils of the same material and thickness as the target foils. The titanium filter for the titanium target and the copper filter for the copper target were installed perpendicularly to the electron beam at the exit of the lead collimator. The idea is that such filter should sufficiently absorb x-ray radiation with energies near the *K*-edge, which could ionize the target atoms' *K*-shell.

Measured *K*-shell ionization cross sections found with the use of equations (1,2) for both front and back target surfaces by both detectors are presented in table 2 for titanium atoms and in table 3 for copper atoms. The cross sections obtained with installed filters are *italicized*. One can see that the cross sections measured with and without filters are practically the same, within errors.

Despite the fact that the x-ray filters do not noticeably affect the measurement results, the cross sections measured from the front surface of the target exceeds the ones measured from the back surface. In the case of titanium target (see table 2) this is quite reasonably explained by the influence of TR generated by the incident electrons on the front surface of the target, as well as in the filter or Kapton foil [15–19].

However, the corresponding increased (compared to the result obtained from the observation of CXR from the back surface) value of the cross section for the copper target (see table 3) is too high and cannot be explained just by the effect of TR. Such high values of the cross sections can be due to additional irradiation of the copper target front surface by the accompanying radiation that passed through the filter and with high values of the atomic concentration and photoionization cross section in the wide range of x-ray photon energies (which are 1.5 and 2.5–3.5 times higher than that of the titanium target, respectively) [24]. It should be noted that for the theoretical estimation of the high cross section values corresponding to the front surface of the copper target (which are observed by both detectors for both physical surfaces of the target), additional investigation are required.

Reliable data about electron impact *K*-shell ionization cross section can be found at measurements from the back surface of the target, since the accompanying ionizing radiation is practically absorbed in the target volume.

3.3 Estimation of the measurement uncertainty

Measurement error of the ionization cross section can be calculated using the formula

$$\left(\frac{\Delta\sigma_K}{\sigma_K}\right)^2 = \left(\frac{\Delta\Omega}{\Omega}\right)^2 + \left(\frac{\Delta n}{n}\right)^2 + \left(\frac{\Delta\omega_K}{\omega_K}\right)^2 + \left(\frac{\Delta N_\gamma}{N_\gamma}\right)^2 + \left(\frac{\Delta N_e}{N_e}\right)^2, \quad (3)$$

where

$$\left(\Delta N_\gamma\right)^2 = \sum_{i=\alpha,\beta}\left(N_\gamma^i\right)^2 \left\{\left(\frac{\Delta N_{\gamma\exp}}{N_{\gamma\exp}}\right)^2 + \left(\frac{\Delta T_{air}}{T_{air}}\right)^2 + \left(\frac{\Delta\varepsilon^i}{\varepsilon^i}\right)^2 + \left(\frac{\Delta\lambda^i}{\lambda^i}\right)^2 + 2\frac{\left(\Delta d/\lambda^i\right)^2 + \left(d\,\Delta\lambda^i\right)^2/\left(\lambda^i\right)^4}{1-\exp\left[-\sqrt{2}d/\lambda^i\right]} e^{-2\sqrt{2}d/\lambda^i}\right\} \quad (4)$$

includes all the parameters from equations (1,2) and their uncertainties. The main sources of errors include uncertainty of the detector solid angle $\Delta\Omega$, statistical uncertainty of the measured CXR photons numbers $\Delta N_{\gamma\exp}$, and uncertainty of the fluorescence yields $\Delta\omega_K$, as presented in table 4. Contribution of other errors can be neglected.

Table 4. Influence of the main sources of errors on the relative uncertainty of the *K*-shell ionization cross sections of titanium and copper atoms for XR100SDDfast (SDD) and XR100CR (CR) detectors (in %).

Quantity	Titanium target		Copper target	
	SDD	CR	SDD	CR
Ω	6.9	6.5	6.9	6.5
$N_{\gamma\exp}^i$	3.7–4.3	4.2–5.8	2.2–3.7	2.7–4.3
ω_K	3.7		3.7	

Table 5. Average values of the electron impact *K*-shell ionization cross section obtained in this work.

E_0 (GeV)	σ_K (b)	
	Titanium	Copper
1	752 ± 94	343 ± 24
2	889 ± 85	386 ± 35

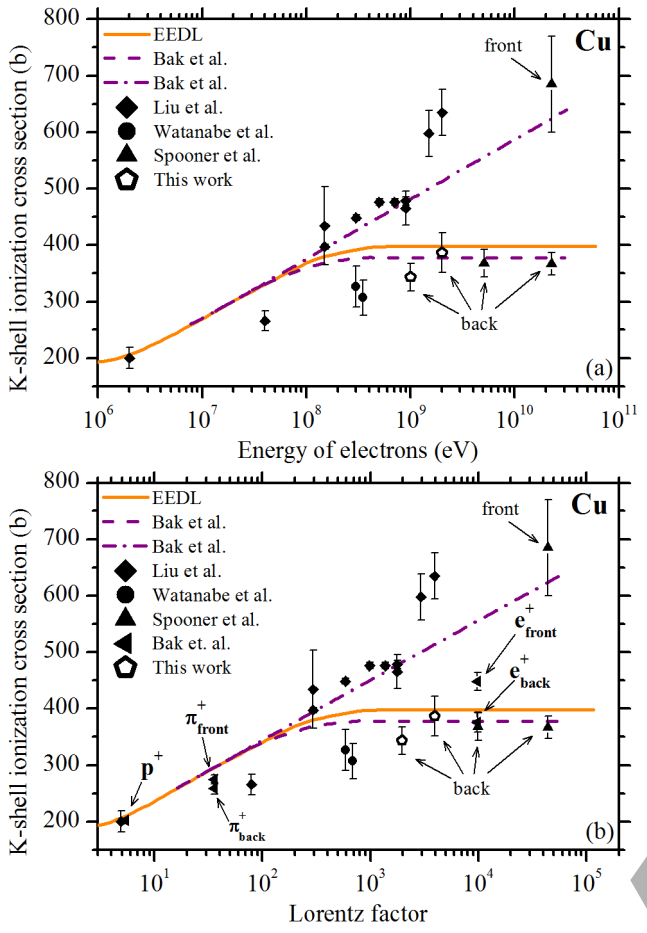

Figure 4. Dependence of the *K*-shell ionization cross section of copper atoms (a) on the electron energy and (b) on the Lorentz factor of incident charged particles (open pentagons are experimental data from this work (table 5), solid markers are experimental data from references [15,19,26,27], lines are calculations from references [14,28]).

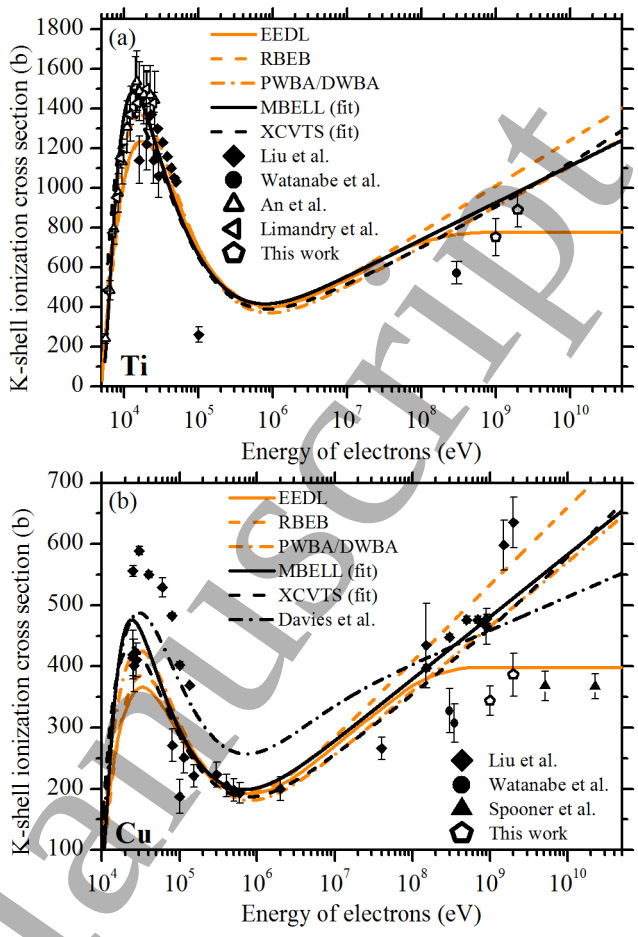

Figure 5. Comparison of the measured dependence of the *K*-shell ionization cross section of (a) titanium and (b) copper atoms on the electron energy with the results of calculations (open pentagons are experimental data from this work (table 5), other markers are experimental data from references [19,26,27,31,32], lines are calculations from references [6,28,33–36]).

Since the values of solid angles did not change during the measurements, their uncertainty is systematic, as is the uncertainty in the fluorescence yield. It can be noted that there may be significant discrepancies between the experimental data for fluorescence yields $\Delta\omega_K$ (collected and analysed by Kahoul et al. [25]).

The final results of the measured electron impact *K*-shell ionization cross sections are presented in table 5. The results are derived by averaging the cross sections obtained from the analysis of x-ray spectra measured by both detectors. In this case, only CXR emitted from the back surfaces of the targets was taken into account.

4. Discussion

Interest in measuring the ionization cross sections of atoms by relativistic charged particles is associated with the possibility of saturation of the cross section at high energies due to the density effect. Figure 4 shows a comparison of the *K*-shell ionization cross sections of copper atoms obtained in the present experiment (table 5) with the experimental data collected and reevaluated by Liu et al. [26], measured by Watanabe et al. [27], Spooner et al. [19], Bak et al. [15], as well as with the results of calculations from reference [14] and from Evaluated Electron Data Library (EEDL), combining the modified Møller binary collision cross section, the modified Weizsacker-Williams method and the density-effect correction [28]. Experimental data provided by Bak et al. [15] correspond to the ionization cross sections by protons (p^+), pions (π^+) and positrons (e^+) with momentum of 5 GeV/c. The experimental data from references [15,19] are presented both for front and back surfaces of the targets. The presented results from reference [14] were obtained by calculations with (dashed line) and without (dash-dotted line) taking into account the density effect influence.

It can be noted that the experimental data were divided into regions with saturated and unsaturated cross sections.

This feature confirms the assumption that the density effect in its pure form can be observed applying the radiation from the back surface of thick targets [19]. In the ultrarelativistic case, the density effect significantly reduces the values of the cross section expected for an isolated atom. This should be considered, for example, when modeling the interaction of charged particles with the condensed matter.

At the moment, there is a large amount of experimental data, as well as theoretical and semi-empirical models for calculating the ionization cross sections of atomic shells of various elements [29,30]. Figure 5 shows all available experimental values of the electron impact *K*-shell ionization cross sections of titanium and copper atoms provided by Liu et al. [26], Watanabe et al. [27], An et al. [31], Limandri et al. [32], and Spooner et al. [19]. The experimental data are compared with calculations based on: EEDL [28], relativistic binary-encounter Bethe model (RBEB) [33], combination of plane-wave Born approximation and distorted-wave Born approximation (PWBA/DWBA) [34], fits based on the Belfast ionization model (MBELL) [35], fits extending the CVTS model (XCVTS) [36], and a fit suggested by Davies et al. for copper atoms [6].

Large discrepancies between experimental data obtained by different authors, as well as between theoretical models, require additional measurements, especially at high energies of incident particles.

5. Conclusion

K-shell ionization cross sections of titanium and copper atoms by electrons with energies of 1 and 2 GeV were measured in this work. New data obtained for copper are in agreement with the calculations, which take into account saturation of the cross section due to the density effect [14], and also with the saturated cross section value measured by other authors [15,19] for different energies of incident charged particles. New data obtained for titanium are close to the saturated cross section provided by EEDL [28].

The ability to observe the density effect is due to the used scheme for measuring the cross sections by analysing the spectra of CXR emitted from back surfaces of the targets. Also, such a measurement scheme made it possible to reduce the influence of radiation background generated by the primary electrons in the beam line equipment and in the target on the measurement results.

Acknowledgements

The work was partially supported by the project AIDA-2020 (TA) within the European Union's Horizon 2020 research and innovation program under grant agreement No 654168. The measurements leading to the presented results have been performed at the Test Beam Facility at DESY Hamburg (Germany), a member of the Helmholtz Association (HGF). The work of R.M.N., A.V.S., and A.S.K. was financially supported by a Program of the Ministry of Education and Science of the Russian Federation for higher education establishments, project No. FZWG-2020-0032 (2019-1569). The work of A.P.P., A.S.G., and N.A.F. was supported by the Ministry of Education and Science of the Russian Federation Grant #FSWW-2020-0008.

References

[1] Furlanetto S R and Stoever S J 2010 *Mon. Not. R. Astron. Soc.* **404** 1869–1878
[2] Winstead C and McKoy V 2000 *Adv. At., Mol., Opt. Phys.* **43** 111–145
[3] Stawarz Ł, Petrosian V and Blandford R D 2010 *Astrophys. J.* **710** 236–247
[4] Adriani O et al. (CALET Collaboration) 2017 *Phys. Rev. Lett.* **119** 181101
[5] de Avillez M A, Guerra M, Santos J P and Breitschwerdt D 2019 *Astron. Astrophys.* **631** A42
[6] Davies J R, Betti R, Nilson P M and Solodov A A 2013 *Phys. Plasmas* **20** 083118
[7] Nilson P M et al. 2012 *Phys. Rev. Lett.* **108** 085002
[8] Plante I and Cucinotta F A 2009 *New J. Phys.* **11** 063047
[9] Nazhmudinov R M, Kubankin A S, Karataev P V, Kishin I A, Vukolov A V, Potylitsyn A P, Zhukova P N and Nasonova V A 2018 *J. Instrum.* **13** P12012
[10] Chaikovska I, Chehab R, Artru X and Shchagin A V 2017 *Nucl. Instrum. Methods Phys. Res. B* **402** 75–78
[11] Dangerfield G R 1973 *Phys. Lett.* **46A** 19–20
[12] Kamiya M, Kuwako A, Ishii K, Morita S and Oyamada M 1980 *Phys. Rev. A* **22** 413–420
[13] Genz H, Brendel C, Eschwey P, Kuhn U, Löw W, Richter A, Seserko P and Sauerwein R 1982 *Z. Phys. A: At. Nucl.* **305** 9–19
[14] Bak J F, Meyer F E, Petersen J B B, Uggerhøj E and Østergaard K 1983 *Phys. Rev. Lett.* **51** 1163–1166
[15] Bak J F, Petersen J B B, Uggerhøj E, Østergaard K, Møller S P and Sørensen A H 1986 *Phys. Scr.* **33** 147–155
[16] Sørensen A H 1987 *Phys. Rev. A* **36** 3125–3137
[17] Cheehin V A and Ermilova V K 1989 *Z. Phys. D: At. Mol. Clusters* **13** 33-43
[18] Meyerhof W E, Jensen D G, Kawall D M, Kuhn S E, Spooner D W, Meziani Z-E and Faust D N 1992 *Phys. Rev. Lett.* **68** 2293–2296
[19] Spooner D W, Meyerhof W E, Kuffner J J, Montenegro E C, lshii K, Kuhn S E, Kawall D M, Jensen D G and Meziani Z-E 1994 *Z. Phys. D: At. Mol. Clusters* **29** 265–268
[20] Diener R, Dreyling-Eschweiler J, Ehrlichmann H, Gregor I M, Kötz U, Krämer U, Meyners N, Potylitsina-Kube N, Schütz A, Schütze P and Stanitzki M 2019 *Nucl. Instrum. Methods Phys. Res. A* **922** 265–286
[21] Deslattes R D et al. *NIST Standard Reference Database Number 128* (National Institute of Standards and Technology, Gaithersburg MD, 20899) https://doi.org/10.18434/T4859Z
[22] Yashoda T, Krishnaveni S and Gowda R 2005 *Nucl. Instrum. Methods Phys. Res. B* **240** 607–611
[23] Henke B L, Gullikson E M and Davis J C 1993 *At. Data Nucl. Data Tables* **54** 181–342

[24] Berger M J, Hubbell J H, Seltzer S M, Chang J, Coursey J S, Sukumar R, Zucker D S and Olsen K *NIST Standard Reference Database Number 8* (National Institute of Standards and Technology, Gaithersburg MD, 20899) https://doi.org/10.18434/T48G6X

[25] Kahoul A, Abasii A, Deghfel B and Nekkab M 2011 *Radiat. Phys. Chem.* **80** 369–377

[26] Liu M, An Z, Tang C, Luo Z, Peng X and Long X 2000 *At. Data Nucl. Data Tables* **76** 213–234

[27] Watanabe Y, Kubozoe T, Tomimasu T, Mikado T and Yamazaki T 1987 *Phys. Rev. A* **35** 1423–1425

[28] Perkins S T, Cullen D E and Seltzer S M 1991 *Tables and graphs of electron-interaction cross sections from 10 eV to 100 GeV derived from the LLNL Evaluated Electron Data Library (EEDL), Z = 1–100* (United States: N. p.) Lawrence Livermore National Laboratory Report No. UCRL-50400-Vol.31

[29] Llovet X, Powell C J, Salvat F and Jablonski A 2014 *J. Phys. Chem. Ref. Data* **43** 013102

[30] Basaglia T, Bonanomi M, Cattorini F, Han M C, Hoff G, Kim C H, Kim S H, Marcoli M, Pia M G and Saracco P 2018 *IEEE Trans. Nucl. Sci.* **65** 2279–2302

[31] An Z, Liu M T, Fu Y C, Luo Z M, Tang C H, Li C M, Zhang B H and Tang Y J 2003 *Nucl. Instrum. Methods Phys. Res. B* **207** 268–274

[32] Limandri S P, Vasconcellos M A Z, Hinrichs R and Trincavelli J C 2012 *Phys. Rev. A* **86** 042701

[33] Santos J P, Parente F and Kim Y-K 2003 *J. Phys. B: At. Mol. Opt. Phys.* **36** 4211–4224

[34] Bote D, Salvat F, Jablonski A and Powell C J 2009 *At. Data Nucl. Data Tables* **95** 871–909

[35] Haque A K F, Uddin M A, Basak A K, Karim K R and Saha B C 2006 *Phys. Rev. A* **73** 012708

[36] Haque A K F, Talukder M R, Shahjahan M, Uddin M A, Basak A K and Saha B C 2010 *J. Phys. B: At. Mol. Opt. Phys.* **43** 115201